

whereas the required memory capacity was decreased to 1500–2000 bits. In this case also practically full independence of the variants was obtained. Thus with the seven variants (11–17) paralleled the actual reliability of recognition—98.5%, whereas calculation gives 98.3%.

Thus the machine effectively learned to recognize the patterns used in the experiment—the numerals 0, 1, 2, 3, and 5. As already mentioned, no information on the properties of these patterns was contained in the program, and, therefore, this machine is in principle capable of learning to distinguish a broad class of other fairly simple patterns.

**Analysis of Reliability of Systems with Fault Signaling, V. A. Zhozhikashvili and A. L. Raikin, pp. 352–357.**

Indices of reliability of systems are given when the probabilities of the system in use at any arbitrary time instant have been taken into account; the fact that the occurrence of some faults is signaled is also taken into account. Various kinds of operational servicing of the system are examined. An example is given to illustrate the proposed procedure.

*Conclusions:*

1) The reliability index of a system when checking and signaling of faults takes place is obtained by extending the usual meaning of reliability of a continually operating system. The probability of failure is now also related to its probability of being in use.

2) Similar indices may prove useful when determining or selecting methods of increasing the reliability of a system or its operation policy.

3) From the examination of the expression given, one observes that in an actual example the average value between successive failures of the system also depends on the transition intensity of the system to the used state, and also on the replacement intensity of the regularly checked faults. In the limit, by making the average repair time approach zero, the maximum average time between failures can be obtained, the latter depending only on the system's transition intensity to its state of use and the intensity of occurrence, in the system, of faults which are not being regularly checked.

**Volume 23, Number 4, April 1962**

**Relations between Adjoints Corresponding to Elements of a Determinant and Their Application to Invariance Theory, V. D. Vershinin, pp. 401–405.**

The existence of a relationship between the adjoints of a determinant is shown. Thence a formula can be deduced enabling one to evaluate the determinant from its  $n - 1$  adjoints. The mutual dependence of variations of elements is investigated when the value of the determinant remains constant.

**Mapping the Movement of a Digital Servosystem on a Multiplane Phase Surface, V. P. Strakhov, pp. 424–435.**

This paper demonstrates the possibility of analyzing digital servosystems by mapping their dynamics on a multiplane phase surface. A study is made of the behavior of such systems when various typical nonlinearities are present; certain parameter relationships are cited which determine the quality of the transient response.

*Summary:*

1) The movement of a digital servosystem can be mapped on a multiplane phase surface. Such a representation makes it possible to analyze the transient response and to perform the computation of the system parameters.

2) The behavior of a digital servosystem near the equilibrium position is analogous to that of the conventional relay systems.

3) The relationships between the system parameters which are cited in this paper make it possible to relate the transient response quality to the values of the parameter for the analog section of the system and to the characteristic of the feedback pickup unit which performs the quantization of the angular or linear displacement.

4) An analogous method of investigation can be used when the digital servosystem contains nonlinear elements with more complex characteristics that cause undamped oscillations. Under these conditions, it is possible to derive expressions that determine the selection of system parameters on the basis of the conditions governing the absence of periodic movement.

**Canonical Method of Contact Network Synthesis, A. Sh. Blokh, pp. 455–459.**

The conductance function of a contact network consisting of contacts  $x_1, x_2, \dots, x_n$  may be given as a function of the integral intermediate parameter  $s$ , depending in turn on the  $x_1, x_2, \dots, x_n$ . This prescription of the conductance function is, in many cases, more convenient and natural than the traditional form using Boolean functions. Usually the parameter  $s$  is found directly from the verbal description of the operating conditions of the contact network and characterizes the invariant properties of the network. Frequently it is more convenient to introduce several intermediate parameters  $s_1, s_2, \dots, s_m$ .

In the present article, the canonical method of contact network synthesis is studied for the case of intermediate parameters. Intermediate parameters were first considered in another paper, in connection with a matricial synthesis method. The introduction of intermediate parameters reduces the volume of the numerical tree, which leads to a reduction in machine time and permits functions with a larger number of variables to be realized in EDC.

We first note that the conductance of a  $(1, k)$  contact network  $x_1, x_2, \dots, x_n$  is defined by the integral function  $N = f(x_1, x_2, \dots, x_n)$  considering that if  $f(\alpha_1, \alpha_2, \dots, \alpha_n) = \nu$ , the conductance between the input and the  $r$ th output with  $x_1 = \alpha_1$  is equal to unity, and if  $f(\alpha_1, \alpha_2, \dots, \alpha_n) \neq \nu$ , the conductance is equal to zero. If  $N$  is a single-valued function, we term the outputs separated. The conductance of a  $(p, q)$  network is also defined as a function of  $N = f(r, x_1, x_2, \dots, x_n)$ , considering here that if for  $r = i$ ,  $x_i = \alpha_j$ , we have  $f(i, \alpha_1, \alpha_2, \dots, \alpha_n) = \nu$ , the conductance between the  $i$ th input and the  $r$ th output is equal to unity; if  $f(i, \alpha_1, \alpha_2, \dots, \alpha_n) \neq \nu$ , this conductance is equal to zero.

**Harmonic Linearization of Nonlinear Inertial Components of Automatic Systems, E. D. Garber, pp. 484–487.**

The harmonic linearization of certain nonlinear inertial components of automatic control systems is carried out.

**Sensitivity of Hydraulic Nozzle-Flapper Amplifiers, I. M. Krassov, L. I. Radovskii, and B. G. Turbin, p. 491–493.**

The sensitivity of hydraulic nozzle-flapper amplifiers under different operating conditions is analyzed. The basic factors to be taken into account in designing the amplifier and determining the parameters which would make it possible to secure the highest sensitivity under the assigned conditions are presented.

**BULLETIN OF THE ACADEMY OF SCIENCES USSR, GEOPHYSICS SERIES (Izvestiia Akademii Nauk SSSR, Seriia Geofizicheskaya).** Published by American Geophysical Union, Washington, D. C.

**Number 3, March 1962**

**Determination of Some of the Spectral Features of Layered Media, L. L. Khudzinsky, pp. 195–203.**

Consideration is given to an approximate method for determining the frequency characteristics of reflection for heterogeneous layers at near normal incidence and the spectra of the reflected waves corresponding to these layers.

*Conclusions:*

1) A method is suggested for the determination of the frequency characteristic of reflection from a heterogeneous layer with arbitrary distribution of impedance and the spectrum of the reflected wave recorded at the surface.

2) The frequency characteristic of reflection from a heterogeneous layer coincides approximately with the spectrum of the density  $\kappa(t_0)$  of the reflection factor or with the spectrum of the previously differentiated logarithm of the impedance.

3) Two methods of generating pulses of special shape used for approximate determination of the frequency characteristics of reflection from a heterogeneous layer are considered.

4) The multiple pulse generator enables one to obtain periodically repeated trains of narrow square pulses. The generator can be used to determine the frequency characteristic of reflection of a heterogeneous layer consisting of several contacting homogeneous layers. It permits variation of the thickness of one or more of the layers in the heterogeneous layer and of the values of the reflection factors from the sharp interfaces corresponding to this layer.

5) Graphic depiction of the logarithm of impedance is essential for determination of the frequency characteristic of reflection of a heterogeneous layer in which impedance is arbitrarily dependent on depth. The trace of  $\ln \gamma(t_0)$  produced by

the variable width method is repeatedly reproduced by the photocopying apparatus in the equipment for frequency analysis and preliminarily differentiated before feeding to the analyzer input.

6) To determine the spectra of reflected waves recorded at the free surface one must have sets of filters, the frequency characteristics of which are the equivalent of the explosion spectra, the spectral characteristics of the medium and those of the recording channel (including the conditions of the seismograph setting). The purpose of these filters is to introduce the required corrections into the  $\kappa(t_0)$  pulse before it is fed to the analyzer input.

**Analytic Continuation of Two-Dimensional Potential Fields, with Applications to Solution of the Inverse Problem of Magnetic and Gravitational Exploration. I**, V. N. Strakhov, pp. 209-214.

The application is considered of the analytic continuation of potential fields in the solution of the inverse problem of magnetic and gravitational exploration. A new formulation is given of the object of the inverse problem. A solution of the analytic-continuation problem is given, which is a generalization of a previously known solution.

**Analytic Continuation of Two-Dimensional Potential Fields, with Applications to Solution of the Inverse Problem of Magnetic and Gravitational Exploration. II**, V. N. Strakhov, pp. 227-232.

Newton series and the Newton integral transform solution of the first problem: the theory of the Newton transform, introduced by the author, is described. A method is given for the determination of the part, facing the  $Ox$  axis, of the convex envelope for the singularities of the function describing the geo-physical field under investigation.

**Distortions of Seismic Pulse Spectra during Analysis**, V. G. Gratsinsky, pp. 233-239.

The paper describes distortions of seismic pulse spectra caused by analyzing only part of the pulse and by displacement of the zero line of the trace.

#### Summary:

1) Analysis of a pulse when any part of it has been removed leads to distortions in the shape of the spectrum, which take the form of an alteration in the ratio between amplitudes and the appearance of false extrema.

2) Distortions of the spectrum can be caused also if the zero line in the pulse to be analyzed is displaced from the true line.

#### Number 4, April 1962

**Analytic Continuation of Two-Dimensional Potential Fields with Applications to the Solution of the Inverse Problem of Magnetic and Gravitational Exploration. III**, V. N. Strakhov, pp. 324-331.

Inversion of the Newton integral transform and solution of the second problem: an inverse is obtained for the integral transform introduced in another paper. This transform, which is a meromorphic function in the whole complex plane, is studied. A relation is obtained between the integral transform and the expansion of the transformed function in a series of inverse factorials.

**Detection of an Extra Mass and the Depth of a Two-Dimensional Body from the Anomaly  $\Delta g$** , E. G. Bulakh, pp. 349-350.

#### Number 5, May 1962

**Strong-Motion Piezoelectric Seismic Detector**, V. M. Fremd, 410-414.

A simplified procedure is given for design calculations for a piezoelectric seismic detector. A prototype of the instrument has been prepared using piezoceramic barium titanate. The results of an experimental study of various circuits for the seismic detector are described.

Fig. 4 shows a cross section of this prototype. Between the inert mass 1 and the bottom of the shell 2 there is a capsule 3. Two piezoceramic plates of barium titanate are fixed in the capsule. The capacitances of the plates are connected in parallel. The casing of the instrument serves as the positive electrode, and the negative electrode 4 is made of brass foil inserted between the plates with a lead passing through an aperture in the wall of the shell to the preamplifier chamber of the instrument. The inert mass is pressed against the capsule of the piezoelectric element by the pressure exerted by a flat membrane spring 5 on a ball 6. Flat springs 7 attached to the inert mass fix it in an axial direction and exclude transverse displacements of the mass. The apparatus

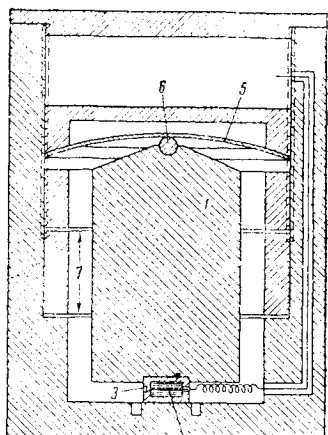


Fig. 4 Cross section of the piezoelectric seismic detector.

can function either as a vertical or as a horizontal seismic detector. *Conclusions:*

1) The simple calculation method proposed makes it possible to construct a family of curves  $P = P(R)$  for different electric loads of a piezoelectric seismic detector and for different assigned parameters  $(\tau, \Delta f, x_{\min}, N_{\text{signal}}/N_{\text{noise}})$ .

2) Analysis of such curves reveals that an electrometric stage with a special tube is most suitable for use as a preamplifier.

3) All the preliminary calculations were confirmed by the experimental data obtained for the prototype seismic detector on a vibroplatform.

4) A piezoelectric seismic detector incorporating barium titanate ceramics and an electrometric preamplifier stage has excellent mechanical and electrical characteristics that permit of its use, in particular, for the magnetic recording of strong motions.

**Some Analytical and Statistical Rules for the Gamma Testing of Naturally Occurring Deposits Containing Radioactive Elements and for Gamma Logging**, D. Savinski, 427-429.

Methods are proposed for decreasing the effect of a nonuniform distribution of radioactive materials, in the operating zone of a detector, on the determination of mean radioactive-element content. It is shown that the method now used yields, for each separate determination, a value of the mean content that is not the best from the probabilistic point of view.

**Experimental Determination of the RaC', ThC", and K<sup>40</sup> Contents of Homogeneous Granitoids from the Gamma-Ray Spectrum**, N. D. Balyasnyi, R. M. Kogan, O. S. Renne, and Sh. D. Friedmann, pp. 430-436.

A scintillation spectrometer was used to obtain spectrograms of  $\gamma$  rays on the surface of homogeneous biotite granites. The distributions of RaC', ThC", and K<sup>40</sup> were measured over a total area of  $\sim 10^4 \text{ m}^2$  (85 points). The zones, with linear dimensions of tens of meters, of RaC' and ThC" concentrations were determined; the average concentrations in zones differ within 20%. The statistical variations of the RaC', ThC", and K<sup>40</sup> distributions in biotite granites satisfy a normal distribution law. The  $\gamma$ -ray spectrum on the surface of granites was calculated.

#### Number 6, June 1962

**Calculation of Magnetic Moments**, A. M. Polonsky, pp. 472-474.

The method of calculating the magnetic moments of bodies from values of the vertical component  $Z$  of the magnetic field in which the remaining integrals need not be taken into consideration is further developed. An arbitrary integration net is considered. The method is generalized for the case of one or more vertical cylindrical bodies of arbitrary cross section with lower edges receding practically to infinity.

$$M = 2R \cdot 0.147 \cdot 10^{-5} \iint Z dS \quad (11)$$

$$h = h_1 + R \cdot 1.85 \left[ 1 - \frac{1}{\sqrt{(1 + R/h_1)^2}} \right] \quad (12)$$

$$2R \cdot 0.147 \cdot 2\pi m (1 - \cos \theta_0) \cos \gamma = IS (h_2 - h_1) \quad (13)$$

$$h_2 = h_1 + R \cdot 1.85 \left[ 1 - \frac{1}{\sqrt{1 + (R/h_1)^2}} \right] \cos \gamma \quad (14)$$

**Conclusions:**

1) Formulas (11), (12), and (18) for the calculation of magnetic moments and of the depths to which they are calculated can be used in the case of one or more vertical or steeply dipping beds of arbitrary cross section with lower edges receding practically to infinity. Thus, for example, the majority of the deposits in the Angara-Il'm iron ore district are of this type. The depths of their upper edges are a few meters below the surface, while the lower edges are at depths of between hundreds to meters and a kilometer or more.

2) These formulas can be used for both vertical and inclined magnetization.

**Theory of Electric Surveying of Buried Structures, A. M. Gluzmann, pp. 489-494.**

A brief review of special coordinate systems is given for the solution of problems on field potential of a current in layered media with interfaces having the form of surfaces of the second order. A solution of a boundary value problem is sought in the coordinate system associated with the boundaries. The method of curvilinear coordinates is used to account for the influence of the shape of the free surface on the field generated by a source located at the boundary of the half space. The solution of the general boundary problem is given for a hyperboloid of revolution.

An interpretation of geophysical observations is based on the solution of the inverse problem in the potential theory by the selection method. To quote a given reference: "Given a certain (wide enough) class of possible structures, the corresponding physical fields are calculated, and 'an admissible' medium is selected as a solution of the problem if the corresponding calculated physical field differs but little from the observed field."

In the electric surveying, the field of electric current observed on the boundary of the half space is the measured physical field. The field characteristics depend on electrical properties of the medium, on the shape of structures, and the free surface as well. Until recent time, the theory of the method of determining the underground structures was based on a limited number of exact solutions of mathematical problems concerning the potential distribution due to a current in an inhomogeneous space. In the present paper we consider a set of boundary value problems in electric surveying which will broaden the interpretation possibilities.

**Theory of Icing of Aircraft, L. G. Kachurin, pp. 526-531.**

The author develops a kinetic theory for the icing of aircraft in supercooled clouds. He investigates the conditions of icing and the structure of an ice coating for various parameters of clouds and flight speeds of the aircraft. Solutions are obtained without considering the spreading of a water film over a surface (one-dimensional case).

**Conclusion:** The developed method for computing the kinetics of the icing of objects in supercooled clouds, together with earlier published methods of aerodynamic calculations for icing, in principle permit us to compute the process of the icing of objects having given aerodynamic characteristics, both for established as well as for unestablished icing conditions.

Under established conditions, the rate of ice accretion equals the rate of arrival of moisture at the object. In an estimation of the time in the course of which there become established the conditions of the aircraft's icing, the flight speed should be taken into consideration. At a speed  $V > 10^4$  cm/sec, the time of the advent of the established conditions will often prove to be of the same order as the time during which the aircraft flies through the most dangerous zone of icing or traverses the zone for which the parameters of the cloud and the flight conditions, and hence the established icing conditions, are maintained.

A further step in the theory of icing can be made in connection with a study of the dynamics of the drops' striking a water-ice surface at high impact velocity (the braking of the drops, their combining with the film and with other drops, the spreading of the film), and in connection with the improvement of the mathematical system for solving the equations (the use of precise data concerning the tangential stress of friction, the assignment of a more general law of heat transfer in a liquid film, a consideration of the film heat exchange with the object, etc.).

At the same time, laboratory tests should be undertaken to refine the developed kinetic icing theory, primarily to clarify the limits of its applicability. Obviously, new interesting results can

be obtained if we introduce into the deliberation, in addition to the viscous and the turbulent conditions of motion, the undulatory conditions of motion as well.

**Effect of Diffusion on the Attenuation of Searchlight Beams, E. M. Feigelson, pp. 532-535.**

An approximate formula is obtained for calculating the effect of multiple diffusion when a searchlight beam passes through a cloud layer.

**Standardization of Photoelectric Measurements of Weak Light Sources, V. M. Morozov, A. D. Bolyunova, and M. A. Ermolaev, pp. 536-539.**

Data are given for alteration in the radiation intensity of FK-106 persistent luminescent compounds in five spectral regions near  $\lambda$  4280, 5280, 5550, 5710, and 5890 Å in relation to alteration in temperature and time. Data are also given for the absolute magnitude of radiation intensity.

**Effect of Polarization on Distribution of the Intensity of Scattered Radiation, T. A. Germogenova, pp. 545-546.**

**Number 7, July 1962**

**Spatial Distribution of Brightness in the Lower Deck Clouds, V. P. Kozlov and E. O. Fedorova, pp. 619-620.**

The experimental data on the directional distribution of cloud brightness are presented. The study of diffusion of light by the

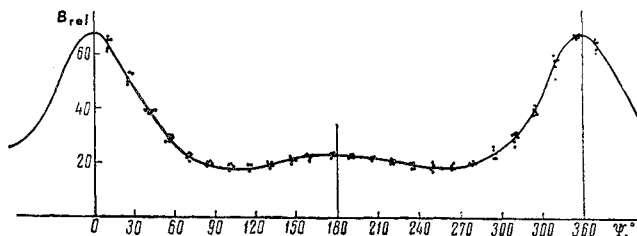


**Fig. 1 Example of direct measurement of azimuthal relationship of cloud brightness Oct. 17, 1960 ( $\theta = 70^\circ$ ).**

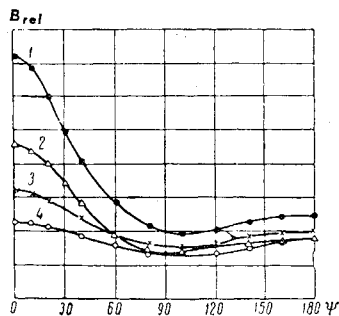


**Fig. 2 Spatial indicatrix of cloud brightness, measured Oct. 17, 1960: 1)  $\theta = 70^\circ$ ; 2)  $\theta = 60^\circ$ ; 3)  $\theta = 50^\circ$ ; 4)  $\theta = 40^\circ$ .**

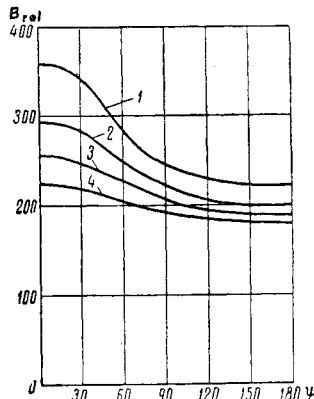


**Fig. 3 Spatial indicatrix of cloud brightness, from Ref. 1: 1)  $\theta = 70^\circ$ ; 2)  $\theta = 60^\circ$ ; 3)  $\theta = 50^\circ$ ; 4)  $\theta = 40^\circ$ .**

clouds is an important and at the same time the most complex problem of atmospheric optics. The complexity of the theoretical analysis of light diffusion in the clouds is caused mainly by a large anisotropic diffusion by an elementary volume. An increase

of the anisotropic light diffusion by an elementary volume, as is known, causes the necessity of considering a large number of terms in the expansion of the scattering function by Legendre polynomials, which in turn with the existing methods of solution complicates the mathematical operations.

Since the scattering function of an elementary volume must contain terms of  $10^2$  order in the expansion by Legendre polynomials, then it is clear that solution of the problem of the light diffusion in clouds would require laborious computations. In expanding usually only a few first terms are retained, but the theoretical evaluation of the error due to this is very complicated. Therefore, it is interesting to compare the results of computations with the direct measurements.

**Determination of the Actual Variation of a Field from Its Integral Characteristics**, Sh. A. Gubermann and D. A. Kozhevnikov, pp. 581-586.

A method is derived for the determination of a field that has been measured by an integrating type of device. The Laplace transform is used in this derivation. Applications of the method to several geophysical problems are investigated: the determination of the field of self-polarization potential, the determination of the influence on readings of the length of radioactivity-radiation measuring devices, the determination of the real anomalies from integrating-radiometer readings, etc.

The solution of a wide class of contemporary scientific and technical problems is related to the experimental investigation of various types of fields, such as electromagnetic, gravitational, and temperature fields, elementary-particle fields, etc. In many cases, the dimensions of the measuring devices used to investigate the fields are such that the variation of the fields within the spatial limits of these devices may be neglected, and it may be assumed that each reading is equivalent to an idealized point reading giving the real strength of the field (scintillation counters, gravimeters, and many other instruments, for example). Instruments are often used, however, within which there is considerable variation of the field amplitude.

The need for measuring devices with relatively large dimensions is often due to the necessity of obtaining a signal stronger than the accompanying noise level, and sometimes due to constructional requirements. The readings obtained by such instruments are proportional to a mean through the body of the instrument of the field amplitude, where this mean is determined by the spatial sensitivity of the instrument. When a field has been measured by an integrating device, the features of the real field cannot be obtained directly, even though such information is of definite value. This is characteristic of geophysical investigations where the source distribution must be determined from the configuration of the field in question.

We thus arrive at the problem of obtaining information concerning the actual field, from information on its integral characteristics, the latter having been obtained by measurements with an instrument of finite dimensions.

#### Number 8, August 1962

**Anomalies Associated with Rotations in the Earth's Magnetic Field**, I, S. N. Gorodensky, pp. 679-684.

A method of calculating the magnetic interference associated with small rotations is considered, and the features of such interference are investigated. Methods are available for magnetic measurements that can measure field-strengths of  $0.1 \gamma$  and smaller ( $1\gamma = 10^{-5}$  oe =  $8 \times 10^{-4}$  a/m.)

The realization of this high measuring-device sensitivity when motion is involved, however, is not yet possible in practice, due mainly to the interference associated with rotation. Interference of a similar type is caused by variations of the earth's magnetic field, recorded in a coordinate system fixed relative to the platform experiencing the rotation. These magnetic-field variations can act directly on the measuring element, and can also generate secondary interference-bearing fields caused by eddy currents in the platform or by variations in the magnetization regime of the soft iron.

In the present paper, we describe a method for calculating the magnetic interference associated with rotation that can be used to investigate interference of the type described above in any case of a small spatial rotation, and that can also be used to study certain characteristic features of rotation-induced interference, both in the general case and in the special case of a cylindrical shell. The method we develop can also be useful in questions concerning the generation of magnetic fields of a predetermined

strength and phase to compensate for magnetic interference and in other similar cases.

Our investigation of rotation-induced interference is based on a rotation transformation which enables us to calculate the components of a vector in a displaced coordinate system. These components are calculated by applying a tensor operator formed from Euler angles to the original components.

**Small-Angle Approximation of a Solution of the Equation for Radiation Transfer and Its Refinement**, L. M. Romanova, pp. 709-711.

The author discusses certain properties of the small-angle approximation of a solution of the radiation transfer equation. For refining this approximation, the equation introduced in another paper is used. A solution in the form of an infinite series is obtained; the calculation of each term in this series reduces only to algebraic operations.

**Contribution to the Effect of "Anomalous Transparency,"** G. P. Gushchin, pp. 712-719.

The author shows the extent of error involved in the aerosol hypothesis of the effect of "anomalous transparency." He presents a new explanation of this effect, based on a consideration of the secondary dispersed ultraviolet radiation in the ozone layer during a low Sun. He proposes a new term for the effect considered, namely, the "Rodionov effect."

#### Number 9, September 1962

**Light Scattering in a Stratiform Cloud**, Ye. M. Feigel'son and O. N. Dobrova, pp. 792-796.

An approximate method has been devised for calculating the intensity of scattered light in a cloud layer. Attention is focused mainly on determining the intensity of light reflected from the boundary of a cloud. Comparison with the results of accurate calculations by other authors shows that the method presented here gives practically accurate flux values and makes it possible to determine the intensity of scattered light within a margin of error which increases with asphericity of the scattering functions but does not exceed on the average 20%.

**Diffusion of Radiation in a Plane Layer**, S. D. Gutshabash, pp. 797-800.

The scattering of light in a medium of finite optical thickness is studied under anisotropic scattering conditions. The probability of emission of a quantum from the medium  $p(\tau, \epsilon, \zeta, \varphi, \varphi_0)$  is expressed by some universal functions  $\Phi_1^m(\tau, \pm\eta)$ . The intensity of diffused radiation at the boundaries and the light pattern within the medium, whatever sources of radiation are operating on the medium, are determined with the aid of these functions.

**Application of Kellogg's Method for Calculating the Intensity of Radiation in the Interior of a Scattering and Absorbing Medium**, L. M. Romanova, pp. 807-808.

#### Number 11, November 1962

**Spectrum of a Segment of a Sinusoidal Curve**, V. G. Gratsinskii, pp. 967-969.

The variation in the flux spectrum of a sinusoidal curve is investigated in detail. The frequency of the basic maximum, the amplitude of the spectrum at frequency  $\omega/\Omega = 1$ , and the amplitudes in the region of lateral extrema show a complex relationship to time.

1) With continuous increase in the duration of the sine curve, the position of the principal maximum in the spectrum describes a complex oscillatory curve and does not smoothly approach the frequency  $\omega/\Omega = 1$ .

2) An increase of the amplitude in the spectrum at frequency  $\omega/\Omega = 1$  with time occurs not linearly but follows a complex law which turns into a straight line only with a sufficient number of periods.

3) The contour of the sine curve spectrum has a multitude of maximum values in the plane  $\{\omega/\Omega, k\}$ .

**Carleman Function and Its Application to the Solution of Certain Geophysical Problems**, G. M. Voskoboinikov, pp. 985-991.

The author considers the possibility and the methods of the analytical extension of potential geophysical fields in the vicinity of sources. He also considers a method of computing the successive moments of the distribution of local sources according to Cauchy data (two-dimensional problem). It was demonstrated

that, under certain limitations, an effective method of solving these problems can be derived with the aid of the Carleman function (of a "quenching" function); simultaneously, under the same limitations, a rigorous solution is given for the problem of separating the local and regional geophysical anomalies.

**Measurements of Scattered Radiation from the Sky in the Region from 1 to 3.5  $\mu$  at Heights up to 15-17 km.** E. D. Sholokhova and E. O. Fedorova, pp. 1041-1042.

In the Tashkent area in 1961, we carried out a series of flights of an automatic spectrometer suitable for measuring the brightness index of the sky at heights up to 15-17 km. The spectrometer, with a diffraction grating, was provided with a special rotating adapter, and with this it was possible to measure sky brightness in separate, fixed parts of the spectrum with the azimuthal angle varying through 360°. The receiver was a cooled, lead-sulfide photometer.

The device was lifted by an automatic stratosphere balloon; signals were transmitted to the earth by a radiotelemetric system and recorded on a photographic film.

Measurements were obtained in four parts of the spectrum, corresponding to the absorption bands of water vapor with centers at 1.38 and 2.6  $\mu$ , and to the transparent bands at 1.23 and 2.2  $\mu$  (the spectral width of the slit was 0.084  $\mu$ ). In addition to this, in some flights the apparatus was operated without a diffraction grating but with filters singling out the spectral intervals: from 0.9 to 1.6  $\mu$ , from 1.7 to 3.5  $\mu$ , and from 0.9 to 3.5  $\mu$ .

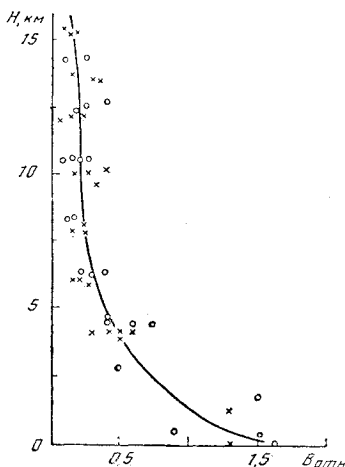


**Fig. 1 Variation of sky brightness with height in the transparent bands of the atmosphere. Azimuthal angle  $\psi = 50^\circ$ , corresponding scattering angle  $50^\circ$  ( $\times \lambda = 2.2 \mu$ ,  $\circ \lambda = 1.23 \mu$ ).**

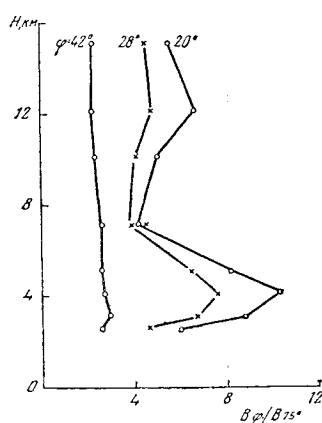


**Fig. 2 Variation of indicatrix elongation with height for various scattering angles  $\varphi$ .**

Examples of the results of measurement are shown in Fig. 1. These show the relative variation of sky brightness with height in the transparent bands at 1.23 and 2.2  $\mu$  (the scales along the horizontal axis for these wavelengths are different). For the transparent bands, there is a characteristic rapid decrease in brightness up to a height of 6-7 km, whereas above this level, within the limits of observation, the variation in brightness is very small. Curves of a similar shape were also obtained for wide spectral intervals, since the sky brightness in this case was determined in practice by the scattering in the transparent bands.

The change in shape of the scattering diagram with height can be followed in the curves in Fig. 2, where the mean values of  $B_\phi/B_{75^\circ}$  for 1.7-3.5 and 0.9-3.5  $\mu$  are shown ( $B_\phi$  and  $B_{75^\circ}$  are the

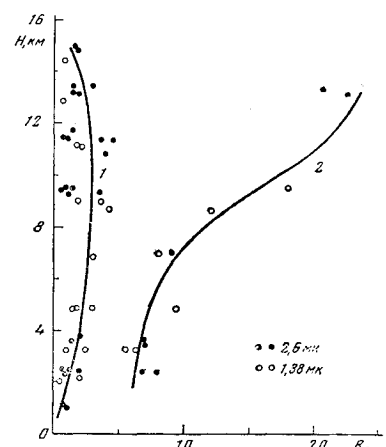


**Fig. 3 Variation of sky brightness with height in the absorption bands of water vapor: 1)  $\varphi = 50^\circ$  ( $\psi = 50^\circ$ ); 2)  $\varphi = 14^\circ$  ( $\psi = 0^\circ$ ).**

brightnesses for scattering angles  $\varphi$  and  $75^\circ$ , respectively). These values characterize the elongation of the scattering diagram. Increases in elongation were observed in the layers of higher turbidity—at about 12 km (the tropopause layer) and at about 4 km. Similar layers of increased turbidity have been previously observed in scattering in the visible region of the spectrum.

In the region of the absorption bands, there is a small increase in brightness relative to that at ground level up to a height of approximately 5 km. The brightness then becomes relatively constant up to the tropopause, and there is then a gradual decrease towards higher levels. This type of variation is characteristic when the angles of scattering are not too small. An example of this behavior can be seen in curve 1 of Fig. 3 ( $\varphi = 50^\circ$ ). For small scattering angles (curve 2 in Fig. 3 for  $\varphi = 14^\circ$ ) a sharp decrease in brightness in the region of the tropopause is observed.

In this case, the observed variation of brightness with height can be explained qualitatively by the dependence of the brightness in the absorption bands on two opposing factors. One of these is the increase with increasing height of the number of scattering particles; the other is the decrease with increasing height of the amount of water vapor, which increases the transparency of the atmosphere.

**Number 12, December 1962**

**Concerning the Effect of Light Scattering in a Real Atmosphere upon the Observed Nightglow Brightness.** V. M. Morozov, pp. 1155-1159.

A statistical analysis of experimental data shows that an increase in the weakening of the direct light of the night sky under a considerable increase in the optical depth of the atmosphere owing to aerosol content is almost entirely compensated by scattered light.

**Spatial Distribution of the Degree of Polarization of Natural Light in the Sea.** V. A. Timofeeva, pp. 1160-1164.

The author has derived a spatial distribution of the degree of polarization of natural light in the sea at various depths in several parts of the visible region of the spectrum. He has determined the effect of the optical depth and the length of the light wave on the spatial distribution of the degree of polarization. He presents a comparison of certain of the derived data with investigations of the polarization of celestial light.

**Number 1, January 1963**

**Some Numerical Methods for Calculating the Second-Order Vertical Derivatives of Potential Fields.** V. N. Strakhov, pp. 65-74.

The rate of convergence of successive approximations to the solutions of integral equations is estimated. Formulas for the numerical calculation of second derivatives, based on approximate solutions containing only one integration (along a straight line or over a plane), are given.

## Number 2, February 1963

Tidal Evolution of the Earth-Moon System, E. L. Ruskol, pp. 129-133.

It is shown that the present observed lag in the tides in the solid body of the earth allows us to construct a consistent picture of the formation of the moon from a swarm of small satellites moving about the earth at distances of 5-20 earth radii, with the subsequent recession of the moon to its present distance being a

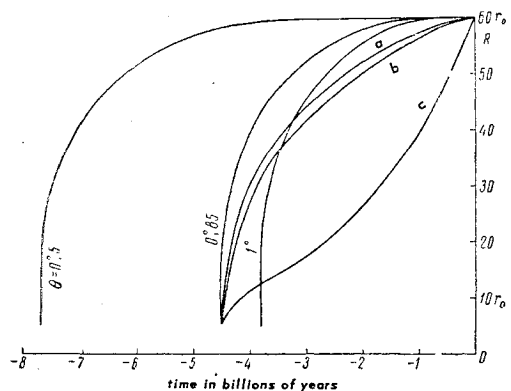
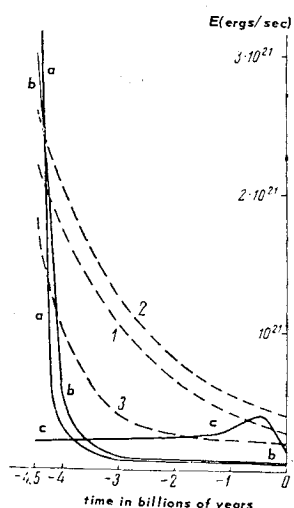


Fig. 1 Change of the earth-moon distance with time for different earth tide lag angles  $\theta$ : a)  $\theta = 1.7^\circ (1 - t/t_{\text{initial}})$ ,  $t_{\text{initial}} = 4.5 \times 10^9$  yr,  $\theta_{\text{present}} = 1.7^\circ$ —; b)  $\theta = 0.05^\circ + \beta (t - t_{\text{initial}})^2$ ,  $\theta_{\text{present}} = 2.1^\circ$ —; c)  $\theta = 0.02^\circ \exp \gamma (t - t_{\text{initial}})$ ,  $\theta_{\text{present}} = 10^\circ$ .

Fig. 2 Generation of heat within the earth by tidal friction (a, b, c refer to cases where the lag angle  $\theta$  changes) and by radioactivity for an earth-moon system age of  $4.5 = 10^9$  yr: 1) radiogenic heat for  $n = 1$  ( $U = 10^{-8}$  gm/gm); 2) the same for  $n = 2$  ( $U = 2 \times 10^{-8}$  gm/gm); 3) radiogenic heat according to Urey.



result of tidal interaction with the earth over a time of 4.5 billion years. An estimate is given of the generation of heat within the earth as a consequence of tidal friction at various epochs, in comparison with the heat generated by the disintegration of radioactive elements.

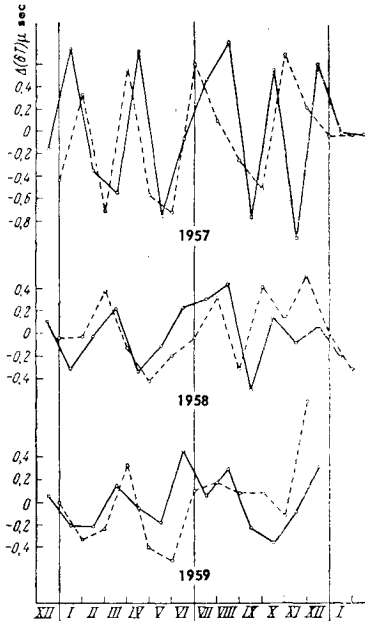
Earth Tides and the Internal Structure of the Earth, N. N. Parfikov, pp. 115-128.

A summary is given of the contemporary state of various methods of studying the tidal deformation of the earth with the object of investigating its internal structure, and determining the Love numbers  $h$ ,  $k$ , and  $l$ . Nine methods of determining the Love numbers are described, and a résumé is given of results (in the form of tables) with estimates of their accuracy. Particular attention is given to the most accurate method—that of measuring the tidal variations of the force of gravity. A formula is derived for the factor  $\delta$  for the tides expressible by spherical harmonics of both the second and third order. The necessity of taking the inertial terms into account is proven. The main results of the theoretical work of M. S. Molodenskii are described, with his results in the theory of static tides and their relation to the internal structure of the earth, and also conclusions from his new dynamic theory of diurnal tides and nutation which takes

the liquid state in the earth's core into account. Results are given of observational dipmeter and gravimeter work carried out recently by the Institute of Physics of the Earth, Academy of Sciences, USSR, that confirm this theory: the difference between the values of  $\delta$  for  $0_1$  and  $K_1$  waves in Tashkent is  $+0.027 \pm 0.003$ . We give a preliminary survey of the determination of the phase lag of earth tides from observations taken by the Institute of Physics of the Earth in Central Asia and from international results, which shows that the tidal lag is approximately 20 min. The reality of this value is discussed and also its geo-physical significance. The main problems of future work in the investigation of earth tides in connection with determining the internal structure of the earth are considered.

Influence of Fluctuations of Atmospheric Circulation of the Earth's Rotation, N. S. Sidorenkov, pp. 234-236.

The earth's atmosphere is constantly in motion relative to its surface because of effects produced by external fields, especially that of solar radiation. Consequently, a constant exchange of angular momentum occurs between the atmosphere and the earth. We shall here consider the effect of this exchange on the rate of the earth's rotation.



Variation of the monthly increments in length of day:  
— Paris Observatory, --- theoretical.

The comparison and analysis of the theoretical and observed characteristics of the earth's rate of rotation lead to the conclusion that fluctuations of atmospheric circulation can evidently account for much of both the annual and irregular variations of the earth's rate of rotation.

BULLETIN OF THE ACADEMY OF SCIENCES USSR, PHYSICAL SERIES (Izvestiya Akademii Nauk SSSR, Seriya Fizicheskaya). Published by Columbia Technical Translations, White Plains, N. Y.

Volume 26, Number 1, 1962

Radiation from Charged Particles Moving Faster Than Light and Its Utilization in the Physics of High-Energy Particles, P. A. Cerenkov, pp. 14-20.

Uses of Luminescence in Biological Research, L. A. Tumerman, pp. 84-92.

Spectral Investigation of the Luminescence of Malignant Tumors, A. V. Karyakin, pp. 93-97.

Volume 26, Number 3, 1962

Use of Computers for Analysis of Crystal Structures, M. A. Porai-Koshits, pp. 328-336.